minerals

MDPI

Article

Accessory minerals in chromitites of Dzharlybutak ore group of Kempirsai massif (Southern Urals, Kazakhstan)

Dmitry E. Saveliev [1]*, Darkhan K. Makatov [2] and Ruslan A. Gataullin [1]

[1] Institute of Geology UFRC RAS, Karl Marks str., 16/2, 450077, Ufa, Russian Federation; savl71@mail.ru
[2] Karaganda State Technical University, Nursultan Nazarbaev av., 56, 100027, Karaganda, Kazakhstan; mdk_geo@mail.ru
* Correspondence: savl71@mail.ru

Abstract: The paper provides results of the mineralogical study of chromium ores from two deposits Almaz-Zhemchuzhina and Geofizicheskoe-VII. It is shown that the main ore minerals are Cr-high spinels (Cr/Cr+Al=0.8–0.83), as well as serpentine and chlorite replacing primary olivine. Chromian spinel grains contain mineral inclusions, which are distributed rather unevenly. The most common inclusion minerals are olivine (serpentine) and amphibole; phlogopite, pyroxenes, and base metal sulfides are rare. Olivine from inclusions in chromite is the highest in magnesium (Fo97–98) and anomalously high in nickel (up to 1.8 wt.% NiO). The closure of exchange reactions between olivine and chromite occurred in the temperature range of 700–850 °C and in the oxygen fugacity range of -1.04 … +2.8 ΔFMQ, which most likely corresponds to the upper mantle settings of the fore-arc basin. A few tens of monomineral and polymineral segregations of platinum group minerals (PGMs) were found in chromite grains. Notably, monomineral segregations are mainly represented by Ru, Os, and Ir disulfides, while in polymineral segregations iridium prevails (with widespread native phases, sulfides, and sulfoarsenides). One of important localization features of the PGM grains is their almost permanent co-existence with hydroxyl-bearing silicates, i.e. amphibole, less often phlogopite or chlorite. Discussed in the paper is the possible genesis of ores and inclusions. It was preliminarily concluded that the subsolidus solid-phase processes played a leading role in chromitites formation.

Keywords: chromitites; Cr-spinel; olivine; amphibole; PGM; ophiolite; ultramafic rock; Kempirsai

Citation: Saveliev, D.E.; Makatov, D.K.; Gataullin, R.A. Accessory minerals in chromitites of Dzharlybutak ore group of Kempirsai massif (Southern Urals, Kazakhstan). *Minerals* **2023**, *13*, x. https://doi.org/10.3390/xxxxx

Academic Editor(s):

Received: date
Accepted: date
Published: date

Publisher's Note: MDPI stays neutral with regard to jurisdictional claims in published maps and institutional affiliations.

Copyright: © 2023 by the authors. Submitted for possible open access publication under the terms and conditions of the Creative Commons Attribution (CC BY) license (https://creativecommons.org/licenses/by/4.0/).

1. Introduction

Kempirsai is one of the largest massifs in the Urals that hosts unique deposits of chromium ores. These deposits are the largest known in ophiolite-type complexes, which reserves are the world's number two after the Bushveld chromite horizons. Ophiolite deposits are often referred to as the so-called podiform deposits due to their irregular morphology, pod-like shape and dunite framing. These features put them in a sharp contrast to reef layers with a persistent strike in platform layered intrusions.

A distinctive feature of most podiform deposits is significant manifestation of secondary processes that affect host rocks mainly (dunites, harzburgites, lherzolites), often completely transforming them into serpentinites and rare chloritolites. Deposits of the Main Ore Field of the Kempirsai massif are not an exception. Here, chromitites are usually framed by dunitic serpentinites, which are then gradually changed by peridotites with abundant bastite pseudomorphs after pyroxenes. Relatively fresh blocks of lherzolites and harzburgites occur sporadically only in boreholes at depths of 300 to 1000 m and deeper. However, serpentinization of ultramafic rocks is usually constrained by the low-temperature stage of mesh serpentine formation, while accessory and ore-forming Cr-spinels are nearly always well preserved and had only minor secondary changes.

The genesis of chromitites of the ophiolite association is still the subject of discussion. Current literary sources commonly interpret it based on the melt+restite reaction [1, etc], less often on fluid-metasomatic replacement [2,3] or solid-phase differentiation [4]. Chromite grains often contain solid inclusions, which are highly diverse in composition. Along with inclusions typical of ultramafic rocks (olivine, pyroxenes, serpentine, chlorite, PGM, awaruite), there are quite many "exotic" inclusions, i.e. amphiboles, phlogopite, carbonaceous phases [3,5]. Currently, the presence of such inclusions makes researchers conclude that fluid-hydrothermal processes took place in the genesis of mineralization all the more often.

Mineralogical features of the chromitites of the Kempirsai massif have been highlighted in many earlier works [6–14] with the limelight given to description of PGM inclusions. The purpose of this work is to characterize mineral inclusions in grains of ore-forming Cr-spinels from one of the most productive ore clusters in the southern Kempirsai massif, i.e. Dzharlybutak. The inclusions are characterized on the example of the core material from wells drilled at the unique Almaz-Zhemchuzhina deposit and minor Geofizicheskoe-VII deposit. Features of localization, morphology and composition of inclusions of various minerals in chromite grains can facilitate interpretation of ore formation processes.

2. Objects and Methods

The study objects were chromitites from two deposits of the Dzharlybutak ore cluster in the Main Ore Field of the Kempirsai massif, i.e. Almaz-Zhemchuzhina and Geofizicheskoe-VII (Figure 1). We studied polished sections of core samples from wells of the Almaz-Zhemchuzhina (750-1100 m deep) and Geofizicheskoe-VII deposits (70–220 m deep), as well as from dumps of the Obyedinenny quarry. A total of 50 polished sections with an area of 30×20 mm was studied. Electron microscopic and compositional studies of minerals were carried out for polished sections and checkers on a Tescan Vega 4 Compact scanning electron microscope with an Xplorer 15 Oxford Instruments energy-dispersive analyzer (IG UFRC RAS, Ufa). The spectra were processed automatically using the AzTec One software package with the TrueQ technique. The following settings were used in the survey: accelerating voltage of 20 kV, probe current in the range of 3–4 nA, spectrum accumulation time at a point 60 seconds in the "Point&ID" mode.

Formulas of olivine and minerals of the spinel group were calculated for 4, those of pyroxenes - for 6 oxygen atoms, respectively. For amphiboles, we made calculations for 23 oxygen atoms by the method described in [15]. In the formulas of the spinel group minerals, the amount of bi- and trivalent iron was determined by stoichiometry. Compositions of olivine and pyroxenes were considered to determine the contents of minals: forsterite (Fo=Mg/(Mg+Fe), at.%), enstatite (En=Mg/(Mg+Fe+Ca), at.%), ferrosilite (Fs=Fe /(Mg+Fe+Ca), at.%), wollastonite (Wo=Ca/(Mg+Fe+Ca), at.%). Abbreviations of minerals that we used in figures comply with those recommended in [16]. Alternatively, the minerals are designated by a formula approximately corresponding to their chemical composition.

3. Results

The Kempirsai ultramafic massif is one of the largest in the Urals. It contains major accumulations of chromium ores confined to rocks of the ophiolite association. The largest podiform chromite deposits are centered in the southeastern part of the massif within the so-called Main Ore Field, where they yield two ore zones (Western and Eastern) and several ore clusters.

The Almaz-Zhemchuzhina deposit is the massif- and world-largest podiform deposit of chromitites with ore reserves of more than 100 million tons at the depth of 1200 m below the surface [17]. It occurs as the thickest (central) branch of the Dzharlybutak ore cluster, which consists of three deposits. The other two branches are the Millionnoye

(western) and Pervomayskoye (eastern) deposits. In the upper part of the ore system, branching bodies of densely disseminated and massive chromitites with a submeridional strike and steep western dip dominate. At the depth of 50-100 m, these bodies merge into a thicker compact deposit with a prevalent massive ores.

The central branch is characterized by a steeper southerward dipping. In the upper part of the deposit, bodies of complex morphology with varying amounts of densely disseminated and massive chromitites dominate. At deeper horizons, the deposits become simpler in shape. They usually occur as gently dipping columnar bodies, turning into a thick, wide and an almost horizontal chromitite deposit [18,19]. To the south, it slightly narrows, while the thickness increases dramatically up to 200 m. Massive and densely disseminated coarse-grained chromitites dominate in the structure of the deposit. The ores are often intersected by thin veins of calcite, amphibole and clinopyroxene composition.

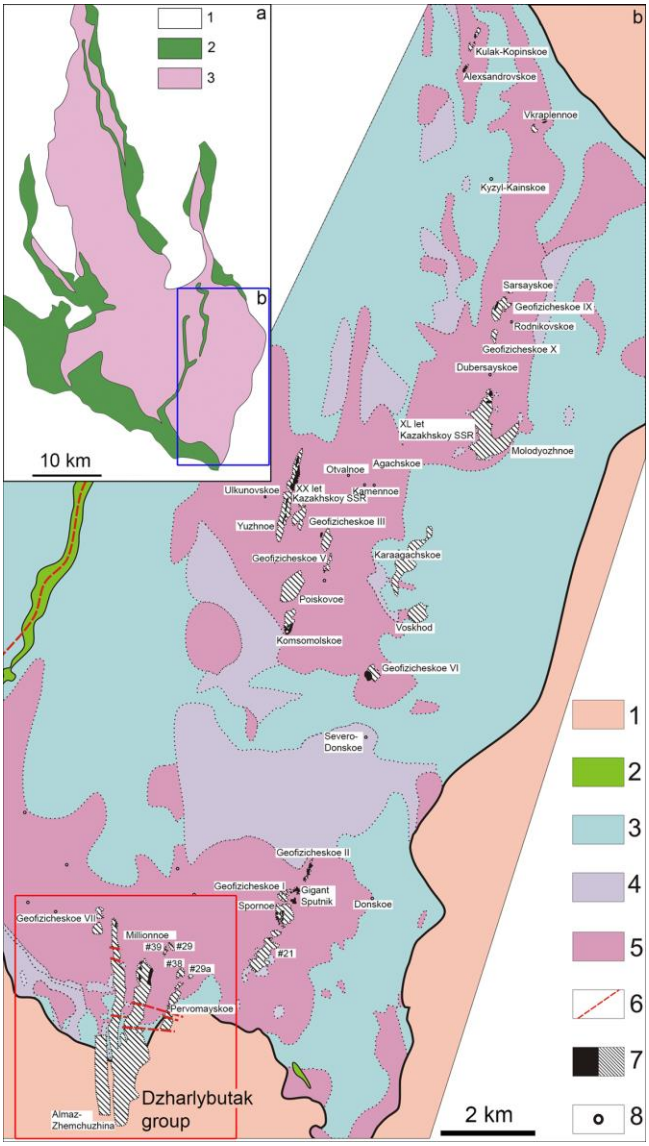

Figure 1. (a) Schematic geological map of the Kempirsai massif and **(b)** geological map of Main Ore Field (after [17,19]). **(a)** 1 – country volcanic and sedimentary rocks, 2 – predominantly igneous and metamorphic mafic rocks of the ophiolite crust section (gabbro, troctolite, pyroxenite, amphibolite), 3 – ultramafic rocks of the ophiolite mantle section; **(b)** 1 – country volcanic and sedimentary rocks, 2 – amphibolite, 3 – predominantly harzburgite, 4 – 5 – dunite-harzburgite unit: 4 – predominantly harzburgite, 5 – predominantly dunite, 6 – faults, 7 – major ore bodies: a – exposed, b – at the depth, 8 – minor deposits and occurrences of chromitites.

The Geophysizeskoye-VII deposit is a small body in the northern part of the Dzharlybutak ore cluster. It occurs close to the surface and has recently been mined and explored in detail. In the structure of the deposit, massive and densely disseminated chromitites dominate, the host rocks are completely serpentinized dunites, bodies of supergene magnesite are occasionally observed.

The studied samples are represented by massive (>90 vol.% of chromite grains) and densely disseminated (70–90 vol.% of chromite grains) chromitites, and only two samples are rare (20–50 vol.%) and moderately disseminated (50–70 vol.%) ore varieties. Textures and structures of chromitites at both studied deposits have similar features: medium-grained (0.5–2 mm) ores dominate, coarse-grained (>2 mm) and fine-grained (<0.5 mm) ores are less common. Textures of the ores are mainly massive and uniform; banding is observed in samples of rare-disseminated chromitites only. Mineral inclusions were found in chromite grains in all of the studied samples (Table 1). Notably, their content rises from disseminated fine-grained to massive ores.

Table 1. Frequency of different minerals in chromitites of Almaz-Zhemchuzhina and Geofizicheskoe-VII deposits.

##	Mineral	Formula	AZH	GVII
1	Cr-spinel	$(Mg,Fe)(Cr,Al,Fe)_2O_4$	+++++	+++++
2	serpentine	$Mg_3(Si_2O_5)(OH)_4$	++++	++++
3	Mg-chlotite	$Mg_5Al(AlSi_3O_{10})(OH)_8$	+++	+++
4	Ca-amphibole	$NaCa_2(Mg_4Al)(Si_6Al_2)O_{22}(OH)_2$	+++	+++
5	orthopyroxene (enstatite)	$MgSiO_3$	+++	–
6	olivine (forsterite)	$(Mg,Fe)_2SiO_4$	++	++
7	clinopyroxene (diopside)	$(Ca,Mg)_2Si_2O_6$	+	–
8	garnet (uvarovite)	$Ca_3Cr_2(SiO_4)_3$	–	+
9	phlogopite	$KMg_3(AlSi_3O_{10})(OH)_2$	+	–
10	zircon	$Zr(SiO_4)$	+	–
11	monazite	$(La,Ce,Nd…)(PO_4)$	+	–
12	apatite	$Ca_5(PO_4)_3(F,OH)$	+	–
13	kassite	$CaTi_2O_4(OH)_2$	+	–
14	pentlandite	$(Fe,Ni)_9S_8$	–	++
15	Co-bearing pentlandite	$(Co,Fe,Ni)_9S_8$	–	+
16	heazlewoodite	Ni_3S_2	++	++
17	millerite	NiS	++	–
18	calcocite	Cu_2S	++	–
19	Native copper	Cu	+	+
20	Native nickel	Ni	+	–
21	awaruite	Ni_3Fe	++	++
22	laurite	$(Ru,Os,Ir)S_2$	++	++
23	erlichmanite	$(Os,Ru,Ir)S_2$	++	++
24	hexaferrum	$(Ru,Os,Ir,Fe…)$	–	+
25	iridisite	$(Ir,Ni,Cu)S_2$	+	-
26	irarsite	$(Ir,Ru,Rh,Os)AsS$	+	+
27	osarsite	$(Os,Ru,Ir)AsS$	+	+
28	unnamed Ni-Cu-Ir_S phase	$(Ni,Cu,Ir,Ru,Os,Rh…)S$	+	–
29	Iridium sulfide	IrS_2	–	+
30	native iridium	Ir	+	+
31	Os-iridium	(Ir,Os)	+	+

32	Ir-osmium	(Os,Ir)	+	+

* +++++ - main mineral (>50%), ++++ - subordinate mineral (10-50%), +++ - accessory mineral, ++ - rare mineral, + - few finding of mineral, – - not detected; AZH – Almaz-Zhemchuzhina, GVII – Geofizicheskoe-VII.

The main ore mineral is chromian spinel, where the content of Cr_2O_3 varies within 57–65 wt.%, Al_2O_3 from 8.2 to 10.56 wt.%, FeO + Fe_2O_3 from 13.5 to 19.31 wt.%, MgO from 13.5 to 14.75 wt.% (Table 2). As for minor elements, significant amounts were found only for TiO_2 (0.16–0.46 wt.%) and NiO (up to 0.24 wt.%), the concentration of the rest is below the detection limit. Massive chromitites produce aggregates of closely intergrown grains, where boundaries of individual crystals are almost indistinguishable. Interstices of ore aggregates are usually filled with secondary silicate minerals, i.e. chlorite or serpentine. The segregation form of these minerals most likely indicates that the silicate material was squeezed out of the ore aggregate during compaction of the latter.

Mineral inclusions in disseminated and massive ores are distributed unevenly. Thus, the vast majority of grains (80%) contains either no inclusions, or as small ones as a few micrometers in size. About 10–15% of the grains contain fairly large single inclusions of olivine, which is currently completely replaced by serpentine. Only 2–5% of the grains show abundant inclusions of other phases, where amphibole is most common, phlogopite is rare (size from a few microns to 50 μm) and occurs in samples from the Almaz-Zhemchuzhina deposit only. As for the inclusions of olivine and amphibole, their distribution, morphology, and preservation are similar in samples from both deposits. Other inclusions (Ni sulfides, awaruite, PGM) are rare and their sizes vary from a fraction of a micrometer to 10–25 μm. Provided below is a detailed description of inclusion minerals.

Olivine in chromite grains is mainly preserved as minor (10–50 μm) rounded and oval inclusions distant from cracks (Fig. 2 a–c). Usually they are intensively developed in chromitites and divide ore grains into separate fragments. However, most of primary olivine inclusions were not preserved, because they were serpentinized during the formation of cracks in the host mineral. Compositionally, relic olivine is high-magnesian (Fo_{95-98}) and contains significant amounts of nickel (0.6–1.8 wt.%). The concentration of manganese above the detection limit was established only in one grain (0.2 wt.% MnO) (Table 3). It should be noted that in the interval of 760–800 m of the Almaz-Zhemchuzhina deposit and in the interval of 120–140 m of the Geofizicheskoe-VII deposit, olivine with anomalous NiO contents (1–1.8 wt.%) is widespread. As the depth increases, the NiO concentration falls to 0.6–0.9 wt.%. A similar phenomenon is observed at the Geofizicheskoe-VII field below and above the indicated interval.

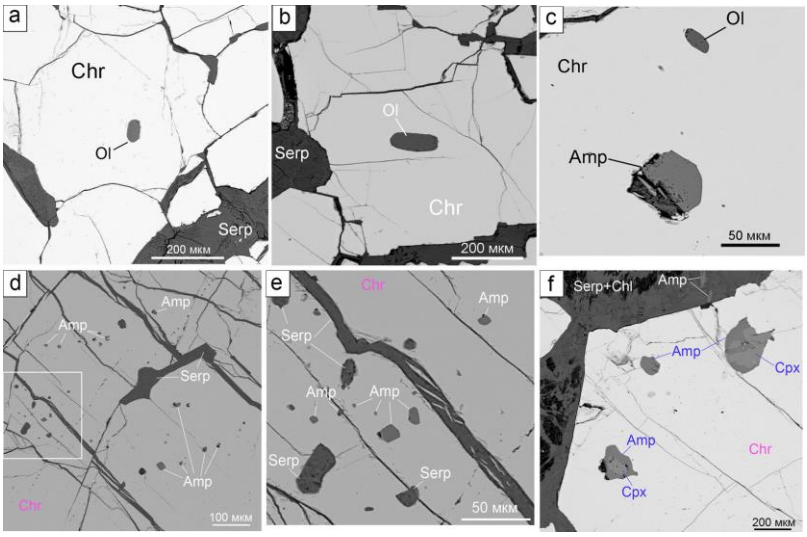

Figure 2. (a) Silicate inclusions in chromitite grains from deposits of Dzharlybutak group. **(a,b)** relic olivine inclusions, **(c)** neighbour inclusions of olivine and amphibole grains, **(d,e)** numerous inclusions of amphibole grains and olivine grains replaced by serpentine, **(d)** general view, **(e)** detailed image, **(f)** inclusions of amphibole grains and intergrowths of amphibole and diopside.

Table 2. Compositions of ore-forming chromian spinels of Almaz-Zhemchuzhina and Geofizicheskoe-VII deposits

#	wt %							Formula coefficients									
	MgO	Al_2O_3	TiO_2	V_2O_3	Cr_2O_3	FeO	NiO	Total	Al	Cr	Mg	Fe^{3+}	Fe^{2+}	Ti	Ni	V	#Cr	#Mg
1	13.39	9.66	0.22	0.00	62.16	15.23	0.00	100.67	0.367	1.582	0.642	0.052	0.357	0.005	0.000	0.000	0.81	0.65
2	13.28	10.32	0.46	0.00	61.97	13.34	0.00	99.53	0.395	1.590	0.642	0.010	0.351	0.011	0.000	0.000	0.80	0.65
3	14.92	8.88	0.20	0.00	63.18	14.58	0.00	101.77	0.332	1.582	0.704	0.081	0.297	0.005	0.000	0.000	0.83	0.70
4	13.46	9.81	0.20	0.00	62.13	14.47	0.00	100.06	0.374	1.587	0.648	0.036	0.351	0.005	0.000	0.000	0.81	0.65
5	13.72	8.79	0.18	0.00	62.64	14.67	0.00	100.00	0.336	1.606	0.663	0.065	0.325	0.004	0.000	0.000	0.83	0.67
6	14.24	9.06	0.18	0.00	62.33	14.56	0.00	100.38	0.343	1.585	0.682	0.061	0.324	0.004	0.000	0.000	0.82	0.68
7	14.33	9.04	0.17	0.00	62.56	14.79	0.18	101.07	0.341	1.580	0.682	0.064	0.324	0.004	0.005	0.000	0.82	0.68
8	14.42	8.64	0.00	0.00	63.13	14.56	0.24	100.99	0.326	1.599	0.688	0.083	0.298	0.000	0.006	0.000	0.83	0.70
9	14.07	8.72	0.19	0.00	62.85	15.44	0.00	101.27	0.329	1.591	0.671	0.079	0.325	0.005	0.000	0.000	0.83	0.67
10	14.09	8.85	0.00	0.00	63.64	15.62	0.00	102.20	0.331	1.597	0.666	0.080	0.325	0.000	0.000	0.000	0.83	0.67
11	14.00	8.73	0.17	0.00	63.08	15.58	0.00	101.56	0.329	1.593	0.667	0.082	0.326	0.004	0.000	0.000	0.83	0.67
12	14.90	8.72	0.16	0.00	63.21	14.46	0.23	101.68	0.326	1.585	0.704	0.078	0.297	0.004	0.006	0.000	0.83	0.70
13	14.70	8.82	0.00	0.00	64.25	14.41	0.00	102.18	0.329	1.606	0.693	0.075	0.297	0.000	0.000	0.000	0.83	0.70
14	14.00	10.56	0.28	0.00	61.03	14.31	0.20	100.39	0.398	1.545	0.668	0.054	0.322	0.007	0.005	0.000	0.79	0.67
15	13.77	9.56	0.23	0.00	62.47	13.74	0.00	99.77	0.364	1.597	0.663	0.019	0.351	0.006	0.000	0.000	0.81	0.65
16	13.62	9.63	0.00	0.00	60.42	14.45	0.00	98.12	0.373	1.570	0.667	0.066	0.324	0.000	0.000	0.000	0.81	0.67
17	13.63	9.51	0.18	0.00	61.57	16.05	0.00	100.93	0.360	1.562	0.652	0.071	0.352	0.004	0.000	0.000	0.81	0.65
18	13.87	9.43	0.00	0.00	62.07	15.04	0.00	100.41	0.358	1.580	0.665	0.072	0.324	0.000	0.000	0.000	0.82	0.67
19	13.65	9.41	0.19	0.00	60.80	15.80	0.00	99.84	0.359	1.557	0.659	0.069	0.352	0.005	0.000	0.000	0.81	0.65
20	14.12	9.36	0.17	0.00	62.91	15.11	0.00	101.68	0.351	1.582	0.669	0.070	0.324	0.004	0.000	0.000	0.82	0.67
21	13.53	9.59	0.16	0.00	61.29	15.26	0.17	100.00	0.366	1.567	0.652	0.055	0.352	0.004	0.004	0.000	0.81	0.65
22	14.22	9.29	0.17	0.00	62.90	15.36	0.00	101.94	0.347	1.577	0.672	0.075	0.324	0.004	0.000	0.000	0.82	0.67
23	15.1	9.29	0.00	0.00	63.01	13.4	0.00	100.9	0.34	1.58	0.71	0.05	0.29	0.00	0.00	0.00	0.82	0.71

	2				9		1	8	3	6	7	5	0	0	0		
24	14.56	9.16	0.17	0.00	64.22	13.94	0.00	102.05	0.341	1.605	0.686	0.040	0.324	0.004	0.000	0.000	0.82	0.68
25	11.53	9.67	0.23	0.00	57.51	19.31	0.00	98.25	0.380	1.515	0.572	0.090	0.438	0.006	0.000	0.000	0.80	0.57
26	13.60	9.37	0.18	0.00	63.12	15.58	0.00	101.86	0.352	1.590	0.645	0.056	0.353	0.004	0.000	0.000	0.82	0.65
27	14.15	8.86	0.18	0.00	64.19	13.28	0.00	100.66	0.335	1.630	0.677	0.029	0.324	0.004	0.000	0.000	0.83	0.68
28	14.15	9.03	0.00	0.00	61.14	13.99	0.00	98.30	0.349	1.584	0.691	0.054	0.323	0.000	0.000	0.000	0.82	0.68

* 1 – 16 – Almaz-Zhemchuzhina, 17 – 28 – Geophizicheskoe-VII. 177

Table 3. Composition of olivine from inclusions in chromite grains of Almaz-Zhemchuzhina and Geofizicheskoe-VII deposits. 178 179

#	wt %									Formula coefficients							
	SiO_2	Al_2O_3	FeO	MgO	CaO	Na_2O	Cr_2O_3	NiO	Total	Si	Al	Fe	Mg	Ca	Na	Cr	Ni
1	53.52	0.76	1.02	17.92	23.96	0.41	1.50	0.00	99.09	1.950	0.033	0.031	0.979	0.935	0.029	0.043	0.000
2	54.09	0.75	1.16	18.32	24.30	0.31	1.07	0.00	100.00	1.951	0.032	0.035	0.991	0.939	0.022	0.030	0.000
3	54.05	0.87	1.22	18.44	24.05	0.27	1.09	0.00	100.00	1.949	0.037	0.037	0.998	0.929	0.019	0.031	0.000
4	54.61	0.29	0.49	18.26	25.97	0.12	0.40	0.00	100.14	1.966	0.012	0.015	0.986	1.002	0.008	0.011	0.000
5	54.78	0.36	0.46	18.32	26.17	0.00	0.32	0.00	100.41	1.968	0.015	0.014	0.987	1.007	0.000	0.009	0.000
6	54.71	0.74	1.10	18.42	24.03	0.40	1.56	0.00	100.96	1.956	0.031	0.033	0.988	0.921	0.028	0.044	0.000
7	57.90	0.38	2.91	37.60	0.24	0.00	0.48	0.20	99.71	1.963	0.015	0.082	1.912	0.009	0.000	0.013	0.006
8	58.29	0.47	2.89	37.38	0.25	0.00	0.41	0.24	99.94	1.974	0.019	0.082	1.899	0.009	0.000	0.011	0.007
9	59.12	0.34	2.66	38.37	0.11	0.00	0.39	0.31	101.30	1.971	0.013	0.074	1.919	0.004	0.000	0.010	0.008
10	59.06	0.43	3.07	37.95	0.31	0.00	0.28	0.20	101.30	1.972	0.017	0.086	1.901	0.011	0.000	0.007	0.005
11	59.10	0.45	2.91	38.52	0.25	0.00	0.34	0.22	101.78	1.961	0.018	0.080	1.917	0.009	0.000	0.009	0.006
12	59.38	0.38	2.93	38.48	0.32	0.00	0.47	0.00	101.96	1.968	0.015	0.081	1.913	0.011	0.000	0.012	0.000
13	59.38	0.36	3.19	38.42	0.24	0.00	0.32	0.22	102.12	1.967	0.014	0.088	1.909	0.008	0.000	0.008	0.006
14	59.53	0.45	3.20	38.20	0.29	0.00	0.35	0.28	102.31	1.970	0.018	0.088	1.897	0.010	0.000	0.009	0.007
15	52.31	2.81	1.85	17.75	22.78	0.00	0.89	0.00	98.19	1.927	0.122	0.057	0.970	0.899	0.000	0.026	0.000
16	53.04	1.42	1.88	18.05	23.41	0.00	0.42	0.00	98.21	1.951	0.061	0.058	0.996	0.922	0.000	0.012	0.000

17	52.61	2.36	1.83	17.73	23.24	0.00	0.86	0.00	98.63	1.929	0.102	0.056	0.975	0.913	0.000	0.025	0.000
18	53.36	1.85	1.88	17.93	23.16	0.00	1.01	0.00	99.18	1.947	0.079	0.057	0.982	0.905	0.000	0.029	0.000
19	52.97	2.13	2.16	17.90	23.17	0.00	0.95	0.00	99.29	1.931	0.092	0.066	0.979	0.905	0.000	0.027	0.000
20	55.20	2.32	5.32	34.58	0.90	0.00	0.51	0.00	98.84	1.910	0.095	0.153	1.795	0.033	0.000	0.014	0.000
21	55.61	2.25	5.45	35.05	0.39	0.00	0.44	0.00	99.19	1.915	0.091	0.156	1.811	0.014	0.000	0.012	0.000
22	55.71	2.23	5.48	35.25	0.39	0.00	0.44	0.00	99.50	1.912	0.090	0.157	1.815	0.014	0.000	0.012	0.000
23	55.74	2.59	5.59	34.87	0.32	0.00	0.60	0.00	99.70	1.913	0.104	0.160	1.795	0.012	0.000	0.016	0.000
24	55.29	3.04	5.53	35.00	0.38	0.00	0.66	0.00	99.89	1.892	0.122	0.158	1.796	0.014	0.000	0.018	0.000

* 1 – 14 – Almaz-Zhemchuzhina, 15 – 30 – Geophizicheskoe-VII. 180

Table 4. Composition of pyroxenes from inclusions in chromite grains of Almaz-Zhemchuzhina and Geofizicheskoe-VII deposits. 181 182

#	wt %								Formula coefficients							
	SiO_2	Al_2O_3	FeO	MgO	CaO	Na_2O	Cr_2O_3	NiO	Total	Si	Al	Fe	Mg	Ca	Na	Cr	Ni
1	53.52	0.76	1.02	17.92	23.96	0.41	1.50	0.00	99.09	1.950	0.033	0.031	0.979	0.935	0.029	0.043	0.000
2	54.09	0.75	1.16	18.32	24.30	0.31	1.07	0.00	100.00	1.951	0.032	0.035	0.991	0.939	0.022	0.030	0.000
3	54.05	0.87	1.22	18.44	24.05	0.27	1.09	0.00	100.00	1.949	0.037	0.037	0.998	0.929	0.019	0.031	0.000
4	54.61	0.29	0.49	18.26	25.97	0.12	0.40	0.00	100.14	1.966	0.012	0.015	0.986	1.002	0.008	0.011	0.000
5	54.78	0.36	0.46	18.32	26.17	0.00	0.32	0.00	100.41	1.968	0.015	0.014	0.987	1.007	0.000	0.009	0.000
6	54.71	0.74	1.10	18.42	24.03	0.40	1.56	0.00	100.96	1.956	0.031	0.033	0.988	0.921	0.028	0.044	0.000
7	57.90	0.38	2.91	37.60	0.24	0.00	0.48	0.20	99.71	1.963	0.015	0.082	1.912	0.009	0.000	0.013	0.006
8	58.29	0.47	2.89	37.38	0.25	0.00	0.41	0.24	99.94	1.974	0.019	0.082	1.899	0.009	0.000	0.011	0.007
9	59.12	0.34	2.66	38.37	0.11	0.00	0.39	0.31	101.30	1.971	0.013	0.074	1.919	0.004	0.000	0.010	0.008
10	59.06	0.43	3.07	37.95	0.31	0.00	0.28	0.20	101.30	1.972	0.017	0.086	1.901	0.011	0.000	0.007	0.005
11	59.10	0.45	2.91	38.52	0.25	0.00	0.34	0.22	101.78	1.961	0.018	0.080	1.917	0.009	0.000	0.009	0.006
12	59.38	0.38	2.93	38.48	0.32	0.00	0.47	0.00	101.96	1.968	0.015	0.081	1.913	0.011	0.000	0.012	0.000
13	59.38	0.36	3.19	38.42	0.24	0.00	0.32	0.22	102.12	1.967	0.014	0.088	1.909	0.008	0.000	0.008	0.006
14	59.5	0.45	3.20	38.2	0.29	0.00	0.35	0.28	102.3	1.97	0.01	0.08	1.89	0.01	0.00	0.00	0.00

	3			0				1	0	8	8	7	0	0	9	7
15	52.31	2.81	1.85	17.55	22.78	0.00	0.89	0.00	98.19	1.927	0.122	0.057	0.970	0.899	0.000	0.026	0.000
16	53.04	1.42	1.88	18.05	23.41	0.00	0.42	0.00	98.21	1.951	0.061	0.058	0.996	0.922	0.000	0.012	0.000
17	52.61	2.36	1.83	17.73	23.24	0.00	0.86	0.00	98.63	1.929	0.102	0.056	0.975	0.913	0.000	0.025	0.000
18	53.36	1.85	1.88	17.93	23.16	0.00	1.01	0.00	99.18	1.947	0.079	0.057	0.982	0.905	0.000	0.029	0.000
19	52.97	2.13	2.16	17.90	23.17	0.00	0.95	0.00	99.29	1.931	0.092	0.066	0.979	0.905	0.000	0.027	0.000
20	55.20	2.32	5.32	34.58	0.90	0.00	0.51	0.00	98.84	1.910	0.095	0.153	1.795	0.033	0.000	0.014	0.000
21	55.61	2.25	5.45	35.05	0.39	0.00	0.44	0.00	99.19	1.915	0.091	0.156	1.811	0.014	0.000	0.012	0.000
22	55.71	2.23	5.48	35.25	0.39	0.00	0.44	0.00	99.50	1.912	0.090	0.157	1.815	0.014	0.000	0.012	0.000
23	55.74	2.59	5.59	34.87	0.32	0.00	0.60	0.00	99.70	1.913	0.104	0.160	1.795	0.012	0.000	0.016	0.000
24	55.29	3.04	5.53	35.00	0.38	0.00	0.66	0.00	99.89	1.892	0.122	0.158	1.796	0.014	0.000	0.018	0.000

* 1 – 14 – Almaz-Zhemchuzhina, 15 – 24 – Geophizicheskoe-VII; 1 –6, 15 – 19 – clinopyroxene; 7 –14, 20 – 24 – orthopyroxene. 183 184 185

Pyroxenes were noted in chromitite samples in a limited amount (Table 4). Orthopyroxene (enstatite) is observed as single inclusions inside chromite grains, but it is best widespread in vein mineral inside veinlets cutting chromitites, where it is often replaced by amphibole. Clinopyroxene (diopside) occurs as rare small prismatic inclusions in chromite (10-25 μm), often in association with amphiboles (Fig. 2 f). Both pyroxenes included in the chromite of the Almaz-Zhemchuzhina deposit are characterized by very low aluminum contents (0.29–0.87 wt.% Al_2O_3), while these values are significantly higher (1.85–3.04 wt.% Al_2O_3) for inclusions from the Geofizicheskoe-VII chromite. The content of titanium and manganese in all studied grains is below the detection limit, sodium is present only in clinopyroxenes of inclusions from Almaz-Zhemchuzhina.

Amphiboles in chromitites are observed in two positions: 1) in the form of primary inclusions in chromite grains and 2) in interstices in association with secondary minerals, i.e. serpentine and chlorite, and the second type was found only in samples from the Almaz-Zhemchuzhina deposit. The composition of interstitial amphibole corresponds to minerals of the actinolite-tremolite or anthophyllite series, while primary amphibole inclusions are always represented by essentially calcium varieties. Notably, amphibole inclusions in chromite grains are the most numerous, with their size ranging from a few microns to 25–30 μm, and their shape varying from tabular to prismatic and acicular (Fig. 2 c–f). Compositionally, the inclusions are fairly consistent and high in magnesium (19.42–23.43 wt.% MgO), calcium (11.24–13.38 wt.% CaO), and permanent impurities of sodium and chromium (0.77–3.14 wt.% Na_2O and 1.56–3.17 wt.% Cr_2O_3). The content of aluminum in the vast majority of analyses (3.58–9.06 wt.% Al_2O_3) is interestingly low. As a result, the studied grains fall into the fields of magnesian hornblende and edenite in the discrimination diagrams (Table 5). Most grains contain an admixture of potassium: usually 0.05–0.2 wt.%, rarely up to 1.07 wt.%.

Alloys, sulfides, sulfoarsenides, Ni, Fe, Cu, and Co arsenides are quite common in the studied samples of chromitites. They often occur in interstices of grains in association with secondary minerals (serpentine, chlorite), less often with amphibole. In chromitites of the studied deposits, sulfides and arsenides of the Ni-Fe-Co-Cu system are represented by small segregations both inside chromite grains and in cracks filled with serpentine. The size of the inclusions varies from a few micrometers to 15–25 μm. The most numerous segregations are represented by heazlewoodite (Fig. 3 a–d), with which segregations of nickeline (Fig. 3 a, b), native copper (Fig. 3 c) and PGMs (Fig. 3 d) can be associated, pentlandite is much less common, in rare cases, cobalt-bearing pentlandite is noted (Fig. 3 e–f). In some segregations of pentlandite, rather high contents of arsenic and the finest segregations of PGMs were revealed. Zonal segregations are noted fairly often (Fig. 3 e); their periphery is composed of awaruite, and the central part is composed of cobalt-bearing pentlandite, reverse relationships were noted less often (Fig. 3 f). In addition, chromitite samples from the Almaz-Zhemchuzhina deposit contain precipitates of millerite and chalcocite (15–25 μm). Some grains of millerite are characterized by the presence of copper impurity (up to 5.45–8.6 wt.%), while all studied heazlewoodite and millerite grains are characterized by low iron contents (<1 wt.%). In some grains of chalcocite, the concentration of iron is increased (up to 10 wt.%). Native minerals are represented by copper with high nickel content (up to 21 wt.%) and almost pure nickel.

PGMs in chromitites of the South Kempirsai deposits were described in many earlier works [6,8,10,14 etc.]. In chromitites of the Dzharlybutak ore cluster, PGMs were found in all studied samples, they are observed exclusively inside chromite grains (Fig. 4) and usually have very small sizes - from fractions of a micron to 3–5 μm, rarely up to 10 μm. At the same time, one interesting feature of PGM segregations in chromite grains in all studied samples is their close association with inclusions of hydroxyl-bearing silicate minerals, i.e. amphibole (Fig. 4 c–e) and rarely chlorite.

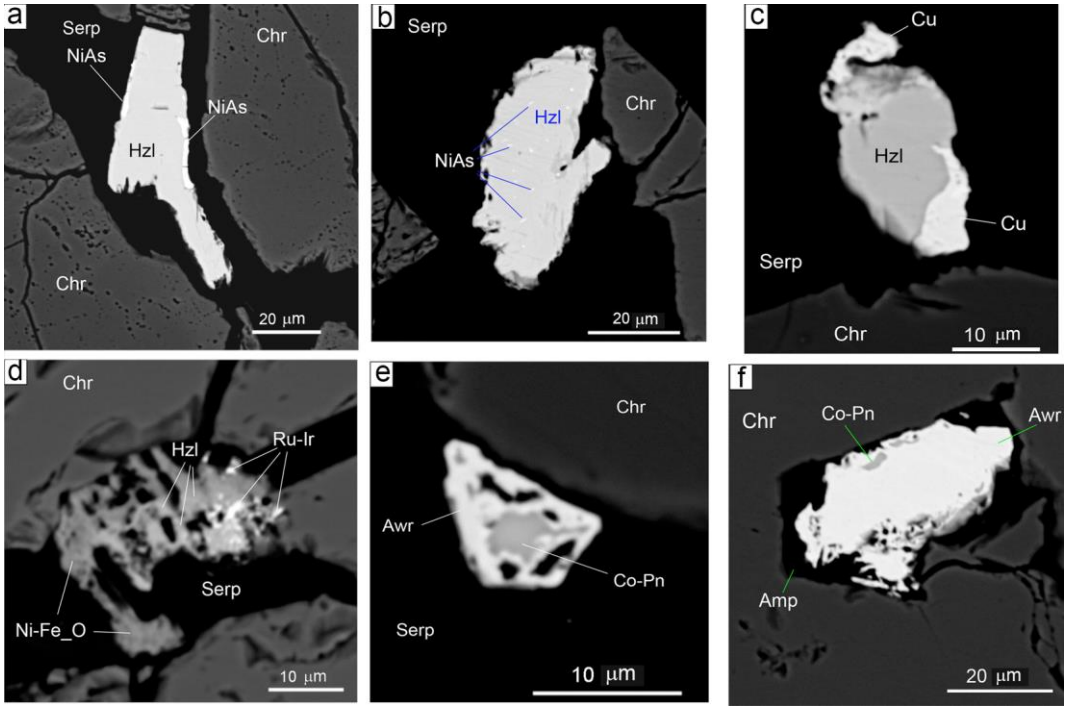

Figure 3. Minerals of base metals (Fe, Ni, Cu, Co) between and into the Cr-spinel grains from the Dzharlybutak group deposits **(a–d)** heazlewoodite grains in serpentine filling cracks in a chromitite aggregate: **(a)** nickeline rim around heazlewoodite grains, **(b)** tiny inclusions of nickeline in heazlewoodite grains, **(c)** native cooper precipitations on the periphery of heazlewoodite grain, **(d)** partly oxidized heazlewoodite grain with tiny PGM inclusions in a chromite grain crack, **(e)** joint of Co-bearing pentlandite and awaruite in the serpentine matrix, **(f)** complex inclusion in the chromite grain that contain amphibole, Co-bearing pentlandite and awaruite.

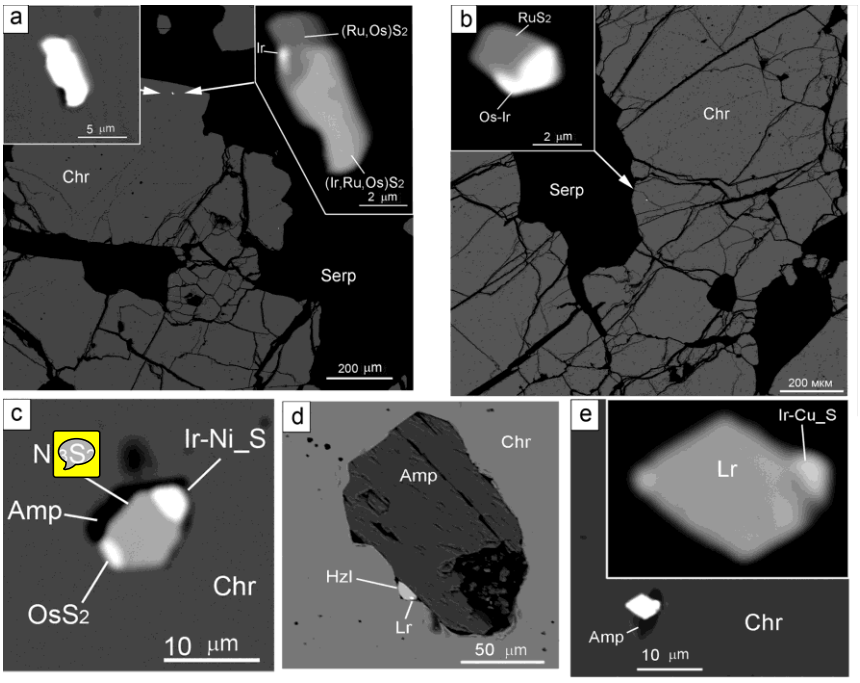

Figure 4. Localization of PGM in chromitites from the Dzharlybutak group deposits **(a)** intergrowth of PGE sulfides with a submicron inclusion of native iridium on the rim of a chromite grain, **(b)** intergrowth of laurite and Os-Ir alloy on the rim of a chromite grain, **(c–e)** PGM inclusions in the central part of chromite grains: **(c)** intergrowth of heazlewoodite, erlichmanite, Ir-Ni-S phase and amphibole, **(d)** microinclusions of heazlewoodite with a laurite precipitation on the rim of an am-

phibole inclusion in a chromite grain, **(e)** small laurite grain with a submicron precipitation of Ir-Cu-S phase associated with amphibole in a chromite grain.

Table 5. Composition of amphibole from inclusions in chromite grains of Almaz-Zhemchuzhina and Geofizicheskoe-VII deposits

#	wt %											Formula coefficients								
	SiO_2	TiO_2	Al_2O_3	FeO	MgO	CaO	Na_2O	K_2O	Cr_2O_3	NiO	Total	Si	AlIV	AlVI	Mg	Fe	Ca	Na	K	Ti	Cr
1	49.60	0.41	7.45	1.35	21.63	13.00	2.35	0.00	2.92	0.00	98.71	6.870	1.130	0.086	4.467	0.156	1.932	0.631	0.000	0.043	0.320
2	49.09	0.22	7.54	1.11	22.04	12.78	2.72	0.10	2.63	0.00	98.24	6.836	1.164	0.073	4.577	0.129	1.910	0.734	0.017	0.023	0.290
3	48.82	0.45	7.34	1.49	21.20	12.48	2.35	0.13	2.89	0.00	97.15	6.875	1.125	0.093	4.452	0.175	1.886	0.641	0.023	0.048	0.322
4	48.76	0.37	7.02	1.14	21.57	12.63	2.34	0.14	2.48	0.02	96.65	6.904	1.096	0.075	4.554	0.135	1.919	0.642	0.025	0.039	0.278
5	50.68	0.47	6.21	1.36	21.68	11.24	1.63	0.00	2.62	0.24	96.13	7.140	0.860	0.072	4.554	0.160	1.700	0.445	0.000	0.049	0.291
6	50.06	0.33	6.95	1.23	21.64	13.38	2.10	0.00	2.72	0.00	98.42	6.943	1.057	0.079	4.476	0.143	1.992	0.565	0.000	0.035	0.298
7	54.06	0.37	3.65	1.47	23.43	11.63	1.05	0.11	1.77	0.00	97.54	7.448	0.552	0.040	4.814	0.169	1.720	0.281	0.019	0.038	0.193
8	53.82	0.24	3.58	1.02	22.58	13.24	0.77	0.25	1.56	0.29	97.35	7.466	0.534	0.051	4.670	0.118	1.971	0.207	0.043	0.025	0.171
9	49.34	0.23	6.96	1.14	22.14	12.87	2.40	0.09	3.08	0.21	98.62	6.872	1.128	0.014	4.598	0.133	1.923	0.648	0.016	0.024	0.339
10	52.24	0.54	4.86	1.05	21.81	12.09	1.25	0.00	2.49	0.30	96.62	7.308	0.692	0.092	4.549	0.123	1.815	0.339	0.000	0.057	0.275
11	51.59	0.56	4.75	1.03	22.14	11.76	1.63	0.00	2.60	0.33	96.38	7.254	0.746	0.041	4.642	0.121	1.774	0.444	0.000	0.059	0.289
12	47.12	0.30	7.93	1.07	21.96	11.75	3.10	0.00	2.78	0.00	96.00	6.721	1.279	0.055	4.670	0.127	1.798	0.857	0.000	0.032	0.313
13	47.14	0.30	8.69	0.95	22.77	12.21	3.25	0.17	3.17	0.00	98.65	6.573	1.427	0.001	4.734	0.111	1.827	0.878	0.029	0.031	0.350
14	49.65	0.30	7.08	1.03	22.21	12.39	2.88	0.00	3.10	0.00	98.64	6.879	1.121	0.035	4.588	0.119	1.842	0.775	0.000	0.031	0.339
15	49.16	0.38	6.93	0.99	22.31	12.17	2.57	0.19	2.76	0.00	97.46	6.887	1.113	0.031	4.660	0.116	1.829	0.699	0.034	0.040	0.306
16	48.60	0.33	7.10	0.94	22.09	12.21	2.84	0.13	2.94	0.00	97.19	6.841	1.159	0.019	4.636	0.110	1.844	0.776	0.023	0.035	0.327
17	49.35	0.25	6.97	0.90	22.37	12.56	2.67	0.00	2.73	0.00	97.80	6.887	1.113	0.033	4.655	0.105	1.881	0.722	0.000	0.026	0.302
18	49.24	0.30	6.99	1.00	22.50	12.25	2.76	0.00	3.03	0.00	98.08	6.860	1.140	0.007	4.675	0.117	1.831	0.746	0.000	0.031	0.333
19	48.81	0.37	7.33	1.00	22.29	12.29	2.66	0.19	2.76	0.00	97.70	6.831	1.169	0.039	4.651	0.117	1.846	0.720	0.034	0.039	0.306
20	48.99	0.42	7.59	1.08	22.06	12.17	2.70	0.00	2.51	0.00	97.51	6.851	1.149	0.102	4.600	0.126	1.826	0.731	0.000	0.044	0.278
21	46.33	0.48	12.92	2.84	19.42	12.52	2.10	0.00	1.89	0.00	98.50	6.448	1.552	0.567	4.030	0.330	1.869	0.567	0.000	0.051	0.207

22	46.36	0.32	9.06	1.21	21.07	13.04	3.14	0.14	3.16	0.23	97.74	6.561	1.439	0.072	4.446	0.143	1.980	0.861	0.025	0.034	0.354
23	47.18	0.31	9.00	1.17	21.64	13.03	3.04	0.11	3.08	0.25	98.80	6.592	1.408	0.073	4.508	0.136	1.953	0.823	0.019	0.033	0.340
24	46.76	0.43	9.64	1.58	21.02	12.24	3.13	0.12	3.08	0.00	98.01	6.567	1.433	0.063	4.402	0.185	1.845	0.852	0.021	0.045	0.342
25	47.71	0.32	7.43	1.11	21.34	12.72	2.43	0.09	2.83	0.20	96.17	6.807	1.193	0.057	4.540	0.132	1.947	0.672	0.016	0.034	0.319

* 1 – 11 – Almaz-Zhemchuzhina, 12 – 25 – Geophizicheskoe-VII.

Table 6. Composition of PGE sulfides from chromitites of Almaz-Zhemchuzhina and Geofizicheskoe-VII deposits

#	wt %										Formula coefficients									
	S	Fe	Ni	Cu	As	Ru	Rh	Os	Ir	Total	S	Fe	Ni	Cu	As	Ru	Rh	Os	Ir	ΣMe
1	31.80	0.85	0.46	0.00	0.00	27.78	0.00	23.97	9.62	94.48	2.00	0.03	0.01	0.00	0.00	0.55	0.00	0.25	0.10	0.95
2	29.30	1.00	0.88	0.00	1.06	12.62	0.00	38.31	13.39	96.60	2.00	0.03	0.03	0.00	0.03	0.27	0.00	0.44	0.15	0.96
3	27.52	0.84	0.47	0.00	0.63	6.98	0.00	45.71	12.89	95.10	2.00	0.03	0.01	0.00	0.02	0.16	0.00	0.56	0.15	0.95
4	27.52	0.68	0.38	0.00	0.00	9.53	0.00	42.51	12.89	93.40	2.00	0.02	0.01	0.00	0.00	0.21	0.00	0.52	0.15	0.93
5	27.94	0.69	0.00	0.00	0.74	9.54	0.00	40.51	14.19	93.61	2.00	0.02	0.00	0.00	0.02	0.21	0.00	0.48	0.16	0.92
6	37.32	0.38	0.00	0.00	0.37	49.66	0.00	5.26	8.64	101.63	2.00	0.01	0.00	0.00	0.00	0.84	0.00	0.04	0.07	0.98
7	31.81	0.44	0.00	0.00	0.00	26.50	0.00	27.11	10.69	96.56	2.00	0.01	0.00	0.00	0.00	0.52	0.00	0.28	0.11	0.94
8	27.68	0.75	0.00	0.00	1.72	17.34	0.69	29.91	4.59	92.60	2.00	0.03	0.00	0.00	0.05	0.39	0.01	0.36	0.17	1.03
9	32.20	0.58	0.28	0.00	0.65	35.34	0.00	15.36	9.14	93.55	2.00	0.02	0.00	0.00	0.01	0.69	0.00	0.16	0.09	0.99
10	33.58	0.57	0.27	0.00	0.00	39.08	0.00	12.28	7.08	92.86	2.00	0.01	0.00	0.00	0.00	0.73	0.00	0.12	0.07	0.95
11	34.08	0.34	0.00	0.00	0.00	35.96	0.00	14.71	12.09	97.16	2.00	0.01	0.00	0.00	0.00	0.66	0.00	0.14	0.11	0.94
12	33.97	0.43	0.00	0.00	0.00	34.62	0.00	15.91	13.29	98.17	2.00	0.01	0.00	0.00	0.00	0.64	0.00	0.15	0.13	0.94
13	33.90	0.39	0.00	0.00	0.00	34.17	0.00	15.81	13.09	97.37	2.00	0.01	0.00	0.00	0.00	0.63	0.00	0.15	0.12	0.93
14	34.46	0.64	0.00	0.00	0.00	39.58	0.00	13.01	7.77	95.46	2.00	0.02	0.00	0.00	0.00	0.72	0.00	0.12	0.07	0.95
15	27.86	0.78	0.00	1.59	1.54	9.47	0.00	39.21	12.79	93.19	2.00	0.03	0.00	0.05	0.04	0.21	0.00	0.47	0.15	0.97
16	32.30	0.72	0.00	0.00	0.00	35.09	0.00	17.40	7.75	93.26	2.00	0.02	0.00	0.00	0.00	0.68	0.00	0.18	0.08	0.97
17	27.29	0.83	0.00	0.00	1.38	8.62	0.00	40.91	13.99	92.95	2.00	0.03	0.00	0.00	0.04	0.20	0.00	0.50	0.17	0.95
18	37.00	0.55	0.00	0.00	0.00	45.60	0.00	9.66	7.45	100.	2.00	0.01	0.00	0.00	0.00	0.78	0.00	0.08	0.06	0.95

	4					2					32	0	7	0	0	0	0	0	8	7	2
19	25.98	1.58	0.00	0.00	1.44	7.25	0.00	44.27	11.56	92.08	2.00	0.07	0.00	0.00	0.04	0.17	0.00	0.57	0.14	1.01
20	29.35	0.83	0.00	0.00	1.02	13.30	0.00	39.92	11.47	95.89	2.00	0.03	0.00	0.00	0.03	0.28	0.00	0.45	0.13	0.93
21	35.19	0.56	0.00	0.00	0.36	36.17	0.00	19.15	9.04	100.47	2.00	0.01	0.00	0.00	0.00	0.65	0.00	0.18	0.08	0.94
22	32.51	0.57	0.00	0.00	0.00	25.60	0.00	27.41	13.42	99.58	2.00	0.02	0.00	0.00	0.00	0.49	0.00	0.28	0.13	0.94
23	28.36	1.83	0.86	0.00	0.38	6.37	1.62	19.03	6.29	94.70	2.00	0.07	0.03	0.00	0.01	0.14	0.03	0.22	0.42	0.94
24	31.36	0.56	0.00	0.00	0.00	27.74	0.00	23.81	10.29	94.31	2.00	0.02	0.00	0.00	0.01	0.56	0.00	0.25	0.10	0.96
25	33.11	0.65	0.00	0.00	0.42	35.41	0.00	17.97	7.98	95.54	2.00	0.02	0.00	0.00	0.01	0.67	0.00	0.18	0.08	0.97
26	36.33	0.00	0.00	0.00	0.50	50.08	2.61	3.58	5.24	98.34	2.00	0.00	0.00	0.00	0.01	0.87	0.04	0.03	0.04	1.01
27	33.65	0.83	0.00	0.00	0.77	38.28	0.00	17.70	6.39	97.62	2.00	0.02	0.00	0.00	0.02	0.72	0.00	0.17	0.06	1.00
28	34.45	0.43	0.00	0.00	0.00	40.98	0.00	12.43	7.90	96.19	2.00	0.01	0.00	0.00	0.00	0.75	0.00	0.12	0.07	0.96
29	35.51	0.52	0.00	0.00	0.00	45.01	0.00	8.98	6.44	96.46	2.00	0.01	0.00	0.00	0.00	0.80	0.00	0.08	0.06	0.96
30	34.34	0.66	0.00	0.00	1.47	39.71	0.00	15.47	6.99	98.64	2.00	0.02	0.00	0.00	0.03	0.73	0.00	0.15	0.06	1.01
31	33.30	0.00	0.00	0.00	1.47	44.36	0.00	6.91	8.66	94.70	2.00	0.00	0.00	0.00	0.03	0.84	0.00	0.07	0.08	1.03
32	36.76	0.00	0.00	0.00	0.00	49.00	0.00	8.76	5.03	99.55	2.00	0.00	0.00	0.00	0.00	0.84	0.00	0.08	0.04	0.97
33	36.48	0.55	0.00	0.00	0.54	50.90	2.17	3.72	4.53	98.89	2.00	0.01	0.00	0.00	0.01	0.88	0.03	0.03	0.04	1.02
34	32.75	0.67	0.25	0.00	0.82	32.75	1.50	16.11	11.89	96.71	2.00	0.02	0.00	0.00	0.02	0.63	0.02	0.16	0.12	1.00
35	36.98	0.00	0.00	0.00	0.00	50.97	1.30	3.26	6.59	99.10	2.00	0.00	0.00	0.00	0.00	0.87	0.02	0.03	0.05	0.98
36	32.00	0.41	0.00	0.00	0.30	35.17	1.33	12.21	11.69	93.04	2.00	0.01	0.00	0.00	0.00	0.69	0.02	0.12	0.12	0.99
37	33.32	0.44	0.00	0.00	0.36	36.36	1.32	12.61	11.79	96.16	2.00	0.01	0.00	0.00	0.00	0.69	0.02	0.12	0.11	0.98
38	33.09	0.00	0.00	0.00	0.00	46.10	1.40	5.81	6.94	93.34	2.00	0.00	0.00	0.00	0.00	0.88	0.02	0.05	0.07	1.03
39	35.06	0.51	0.00	0.00	0.00	49.64	0.00	7.12	6.49	98.82	2.00	0.01	0.00	0.00	0.00	0.89	0.00	0.06	0.06	1.04
40	30.36	1.54	0.00	0.00	1.80	32.58	0.73	15.81	11.69	94.49	2.00	0.05	0.00	0.00	0.05	0.68	0.01	0.17	0.12	1.10
41	32.16	0.00	0.00	0.00	0.99	30.93	1.66	19.01	13.96	96.14	2.00	0.00	0.00	0.00	0.02	0.60	0.03	0.20	0.11	0.98
42	35.88	0.00	0.00	0.00	0.40	49.49	1.86	2.73	6.29	96.65	2.00	0.00	0.00	0.00	0.01	0.87	0.03	0.02	0.05	1.00

* 1– 16 – Almaz-Zhemchuzhina, 17–42 – Geophizicheskoe-VII.

Table 7. Composition of PGE sulfoarsenides from chromitites of Almaz-Zhemchuzhina and Geofizicheskoe-VII deposits

#	wt %											Formula coefficients									
	S	**Fe**	**Ni**	**Cu**	**As**	**Ru**	**Rh**	**Os**	**Ir**	**Pt**	**Total**	**S**	**As**	**Fe**	**Ni**	**Cu**	**Ru**	**Rh**	**Os**	**Ir**	**Pt**	**ΣMe**
1	11.13	0.71	0.00	0.00	30.39	6.93	0.00	47.63	3.19	0.00	99.98	0.924	1.076	0.030	0.000	0.000	0.180	0.000	0.660	0.040	0.000	0.926
2	11.26	0.56	1.10	0.00	28.19	0.00	0.00	0.00	56.28	0.00	97.39	0.967	1.033	0.027	0.052	0.000	0.000	0.000	0.000	0.800	0.000	0.885
3	13.95	1.23	0.57	0.00	21.21	1.19	1.69	0.00	56.02	0.00	95.86	1.213	0.787	0.061	0.027	0.000	0.030	0.046	0.000	0.810	0.000	0.978
4	15.32	0.65	0.25	0.00	19.32	2.22	0.87	6.96	49.05	0.00	94.64	1.300	0.700	0.032	0.012	0.000	0.060	0.029	0.090	0.690	0.000	0.919
5	12.85	0.40	0.00	0.00	33.25	35.65	0.00	6.53	4.59	0.00	93.27	0.951	1.049	0.017	0.000	0.000	0.830	0.000	0.080	0.050	0.000	0.990
6	12.82	0.36	0.00	0.00	33.17	34.36	0.00	8.00	4.91	0.00	93.62	0.951	1.049	0.015	0.000	0.000	0.800	0.000	0.100	0.060	0.000	0.983
7	13.10	1.47	0.00	4.90	24.12	1.26	0.96	3.44	46.93	0.00	96.18	1.120	0.880	0.072	0.000	0.210	0.030	0.020	0.050	0.660	0.001	1.061
8	13.10	1.47	0.00	4.90	24.12	1.26	0.96	3.44	46.93	0.00	96.18	1.120	0.880	0.072	0.000	0.210	0.030	0.020	0.050	0.660	0.001	1.061
9	11.50	1.97	0.00	3.35	21.97	1.12	0.67	3.36	49.38	0.00	93.32	1.100	0.890	0.108	0.000	0.160	0.030	0.020	0.050	0.780	0.001	1.166
10	11.50	1.97	0.00	3.35	21.97	1.12	0.67	3.36	49.38	0.00	93.32	1.100	0.890	0.108	0.000	0.160	0.030	0.020	0.050	0.780	0.001	1.166
11	20.99	0.99	0.93	0.00	17.07	19.59	6.51	4.22	21.87	1.49	93.66	1.485	0.515	0.040	0.036	0.000	0.430	0.140	0.050	0.250	0.010	0.983

* 1– 4 – Almaz-Zhemchuzhina, 5 – 11 – Geophizicheskoe-VII.

In the chromitite samples of the Geofizicheskoye-VII deposit, PGMs compositionally refer to disulfides of the laurite-erlichmanite series with the general formula (Ru,Os,Ir)S_2 and variable ratios between platinum group elements (Table 6). Iridium dominates in composition of some precipitates, and their formula is close to IrS_2. Some segregations are represented by PGE sulfoarsenides compositionally close to irarsite. Solid solutions of PGEs with Ru-Os-Ir-Fe (hexaferrum) composition were found in some chromite grains. Several PGM grains are associated with chlorite. Among other PGEs, laurite–erlichmanite sulfides contain a constant admixture of rhodium in an amount of up to 3 wt.%; in iridium sulfoarsenides, its concentration increases to 5–6 wt.%. In single PGM grains, an admixture of platinum in the amount of 1–2 wt.% is noted, and 1 precipitation of native copper containing 7 wt.% Pt was also revealed. Palladium was not found in the studied minerals.

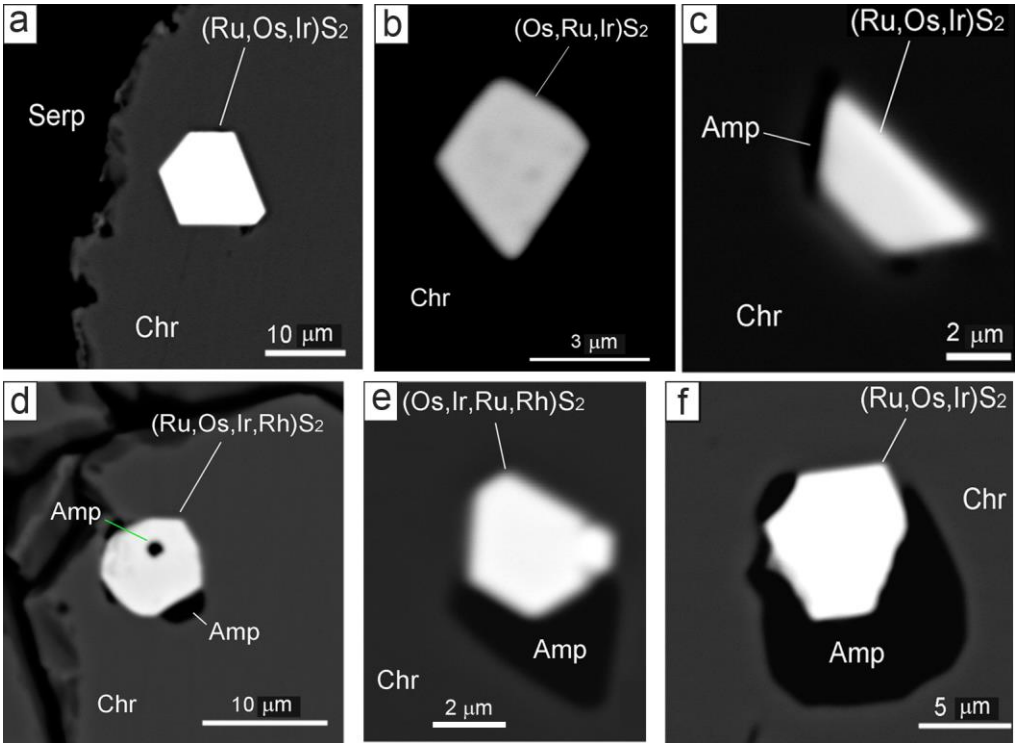

Figure 5. Euhedral grains of laurite-erlichmanite disulfides in chromitites from the Dzharlybutak group deposits **(a,b)** PGE sulfide inclusions in chromite grains, **(c)** laurite inclusion with a fine rim of amphibole in a chromite grain, **(d)** complex inclusion of laurite and amphibole on the periphery of a chromite grain, **(e,f)** laurite-erlichmanite sulfides tightly associated with amphibole grains in chromite grains.

In chromitite samples from the Almaz-Zhemchuzhina deposit, all PGM segregations can be divided into homogeneous (Fig. 5) and polymineral (Fig. 6). Homogeneous precipitates predominate (60%). Compositionally, they refer to disulfides of the laurite-erlichmanite series with the general formula (Ru,Os,Ir)S_2 and variable ratios between PGE. Iridium plays the leading role in polymineral PGM precipitates. Iridium occurs as the following phases: native, osmium iridium, and an essentially iridium sulfide variety, which is calculated for a formula close to iridisite (15%). Sulfoarsenides are represented by both essentially iridium - irarsite (about 10%) and osmium - osarsite (about 10%) varieties (Table 7). Sulfides of complex Ni-Cu-PGE composition (less than 10%) with varying ratios of metals are observed in approximately comparable amounts.

Mineral segregations of the laurite-erlichmanite series typically show a high degree of idiomorphism (Fig. 5). PGM grains are often captured in "amphibole traps" (Fig. 5 c–e) with different areal ratios. Sometimes they contain submicron inclusions of this mineral

(Fig. 5 d). In the structure of PGM polymineral segregations, minerals of the laurite-erlichmanite series are also common and play the main role (Fig. 6 b–d, f, h, i), while inclusions of sulfides, sulfoarsenides and native iridium (or Os-Ir phases, Ir-Os) are secondary (Table 8). In some cases, intergrowths are only represented by iridium minerals of varied composition (Fig. 6 a, e, g). Polymineral segregations of PGM can be tightly associated with amphibole either (Fig. 6 d, i).

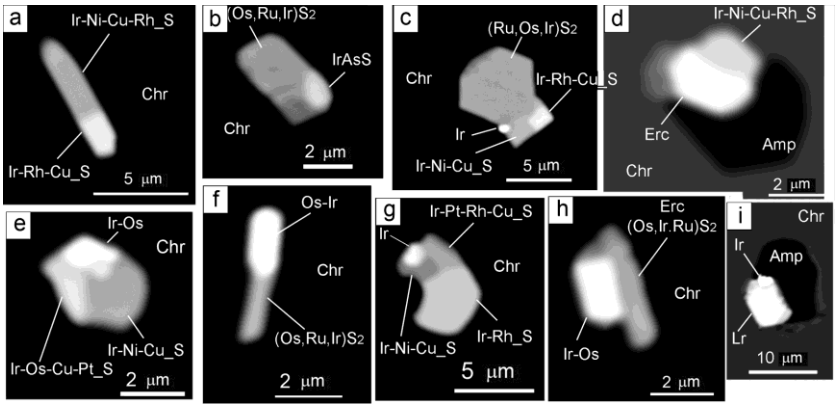

Figure 6. Morphology and internal structure of PGM intergrowths in chromitites from the Dzharlybutak group deposits **(a)** intergrowth of Ir-Ni-Cu-Rh-S and Ir-Rh-Cu-S phases of rod-like morphology in the chromite, **(b)** intergrowth of erlichmanite and irarsite in a chromite grain, **(c)** intergrowth of complex composition (laurite, native Ir, Ir-Ni-Cu-S and Ir-Rh-Cu-S phases) in a chromite grain, **(d)** intergrowth of erlichmanite and Ir-Ni-Cu-Rh sulfide with amphibole in chromite, **(e)** intergrowth of Ir-Os alloy with Ir-Os-Cu-Pt and Ir-Ni-Cu sulfides in a chromite grain, **(f)** rod-like intergrowth of Ir-Os alloy and erlichmanite in chromite, **(g)** four-phase intergrowth of Ir-Ni-Cu, Ir-Rh and Ir-Pt-Rh-Cu sulfides with native Ir in a chromite grain, **(h)** intergrowth of erlichmanite and Ir-Os alloy in chromite, **(i)** intergrowth of laurite and native Ir with amphibole in a chromite grain.

Table 8. Composition of PGE alloys from chromitites of Almaz-Zhemchuzhina and Geofizicheskoe-VII deposits.

#	wt %					Formula coefficients			
	Fe	Ru	Os	Ir	Total	Fe	Ru	Os	Ir
1	0.33	10.70	35.59	45.86	92.48	0.011	0.197	0.348	0.444
2	0.37	10.61	36.16	45.44	92.58	0.012	0.195	0.353	0.439
3	0.60	3.19	41.74	47.27	92.80	0.021	0.062	0.432	0.484
4	0.85	2.87	46.58	42.68	92.98	0.030	0.056	0.480	0.435
5	0.99	3.72	46.86	41.70	93.27	0.034	0.071	0.476	0.419
6	0.67	3.12	41.90	47.59	93.28	0.023	0.060	0.431	0.485
7	0.97	3.50	47.26	42.60	94.33	0.033	0.066	0.476	0.425

* 1– 3 – Almaz-Zhemchuzhina, 4 – 7 – Geophizicheskoe-VII.

In addition to typical minerals of ultramafic rocks and chromitites, in the studied polished sections, we found single segregations of minerals considered "exotic" for these associations, i.e. scheelite, zircon, monazite, apatite, and a Ca–Ti–O phase (presumably, kassite). In order to exclude "artifacts", in Fig. 7 we present pairs of images in different modes – secondary electrons (SE) and back-scattered electrons (BSE). Single segregations of zircon, monazite, and barite were found in chromitite samples from the Almaz-Zhemchuzhina deposit in interstices with serpentine (Fig. 7 a–f). Phlogopite rarely occurs as primary inclusions in chromite grains; it is also more often clustered in interstices in association with secondary minerals (Fig. 7 g–i).

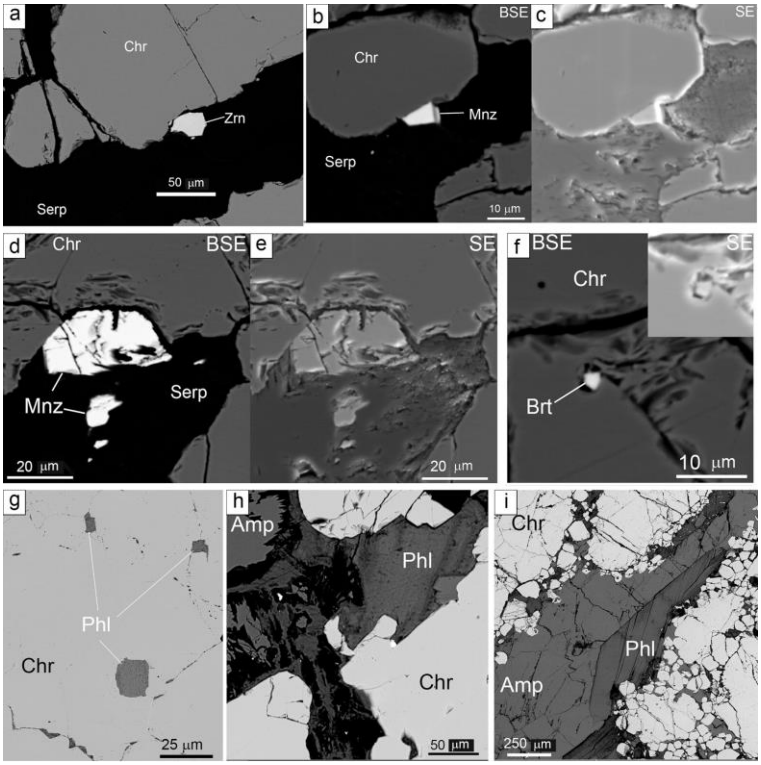

Figure 7. Exotic accessory minerals in chromitites from the Dzharlybutak group deposits **(a)** small zircon grain in a crack filled by serpentine at the boundary with a chromite grain, **(b–e)** euhedral monazite grains in a crack filled by serpentine at the boundary with a chromite grain, **(f)** barite inclusion in a chromite grain, **(g)** phlogopite inclusions in a chromite grain, **(h,i)** phlogopite and amphibole filling cracks in chromitite.

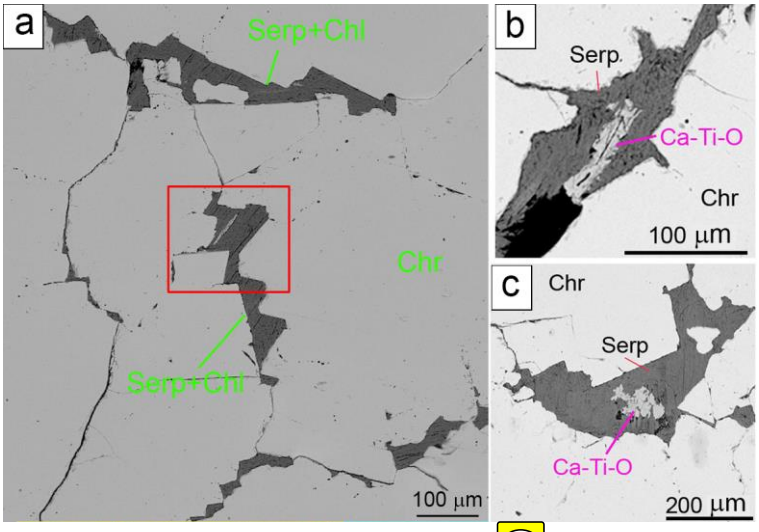

Figure 8. Mineral precipitations of Ca-Ti-O composition in chromitites from the Almaz-Zhemchuzhina deposit **(a)** general view, **(b,c)** detailed images of precipitations of Ca-Ti-O phase.

Apatite was found both as a primary inclusion together with heazlewoodite in chromite and in association with veined amphibole in interstices between ore grains. Sphene is mainly observed in interstices between chromite grains or near cracks, in association with veined amphibole and chlorite. The Ca-Ti-O mineral we found in silicate inclusions in chromite (associated with serpentine and chlorite) (Fig. 8) is not perovskite, since analyses show low amounts and most likely indicate a high hydroxyl content. The

estimation demonstrates its compositional proximity to kassite or cafetite. Kassite was previously described in chromitites of the Saranovsky deposit [20].

4. Discussion

The set of minerals in interstices of ores and inclusions inside chromite grains of the Dzharlybutak ore cluster deposits is generally similar to that of previously studied deposits of the ophiolite type. At the same time, the conducted studies revealed specific compositional features of PGMs, olivine with abnormally high nickel concentrations, as well as the release of minerals rare for ultramafic rocks (zircon, monazite, etc.) in situ, and not only in concentrates.

Such minerals as olivine, serpentine, orthopyroxene, and chlorite are typical of primary or altered ultramafic rocks and their presence is easily interpreted. In particular, the presence of rounded olivine grains in Cr-spinels can be explained by its capture during chromite crystallization either from melts percolating through restite [1] or during syndeformational growth [4].

To determine formation settings of primary mineral associations of chromitites, we calculated the closing temperatures of exchange reactions in olivine-chromium spinel vapors using various versions of geothermometers [21-23], as well as oxygen fugacity for the same pairs of minerals according to the oxybarometer from [21]. The data obtained showed that the formation of chromitite bodies occurred at subsolidus temperatures of ultramafic rocks (700–850 °C) and oxygen fugacity of -1.04 … +2.8 ΔFMQ, which is comparable with previous estimates for the formation of ultramafic rocks in the more northern regions of the Southern Urals [24]. At the same time, the anomalously high content of nickel in olivine indicates an extremely depleted composition, which testifies to the restite origin of ultramafic rocks in the upper mantle of the fore-arc basin [25].

Numerous inclusions of amphibole and phlogopite in chromite are commonly interpreted as a result of either the fluid-metasomatic genesis of chromitites [2], or the reaction of restite with percolating melts and fluids [3,5], "mantle metasomatism" [10]. The main argument here is the very presence of hydroxyl-bearing phases inside unaltered chromite grains. However, in our previous works we used numerous examples to show co-existence of the finest segregations of Cr-spinel and amphibole inside unaltered olivine and orthopyroxene crystals from lherzolites [26]. This may testify to the solid-phase nature of chromite crystallization with inclusions generated by multiple recrystallization inside the plastically deformed mantle material.

PGM mineralization in the studied chromitites is characterized by prevalence of refractory platinoids (ruthenium, iridium and osmium), a subordinate role of rhodium and platinum and the complete absence of palladium. This also complies with formerly obtained data on some deposits in the south-eastern part of the Kempirsai massif [8,14]. Noteworthy, we found no solid solutions with the Rh-Zn-Pt composition, which were reported in [11] for the section of the Almaz-Zhemchuzhina deposit. This may be due to the zonal distribution of PGMs of varied compositions at the deposit and the absence of the mentioned phase in the interval of 750–1100 m, which we studied.

The vast majority of the studied PGM precipitates in chromites is represented by sulfides, while their minor part is alloys (Fig. 9). In contrast to the previously studied chromitites from more northern regions of the Southern Urals (Kraka, Nurali), where laurite predominates [27], the composition of sulfides varies significantly and shows an almost continuous series between essentially ruthenium (laurite) and osmium (erlichmanite) varieties. Interestingly, the role of iridium in the composition of sulfides is rather important. Among native PGM, iridium and an Os-Ir alloy prevail, while proportions of metals are approximately equal, but ruthenium is extremely rare. This fact also distinguishes the studied deposits from those of the Kraka massif.

To explain the genesis of PGM inclusions in chromitites of podiform deposits, several different mechanisms have been proposed in literary sources, depending on the location, morphology, and composition of the inclusions. One of the most comprehensive

reviews on this issue [28] provides a classification of PGM segregations, according to which all the minerals that we studied fall into type I (enriched with IPGE) and occur in inner parts of chromite grains with no visible connection to cracks (subtype 1). The main hypotheses to explain the genesis of these inclusions are usually proposed as follows: 1) incorporation of refractory platinoids into chromite at high mantle temperatures and their separation as own phases upon cooling [29,30]; 2) simultaneous crystallization with chromite from melts or during the melt+peridotite reaction [31,32]; 3) crystallization from fluids and/or melts percolating through ultramafic rocks [10,11], including "supercritical fluids" [8].

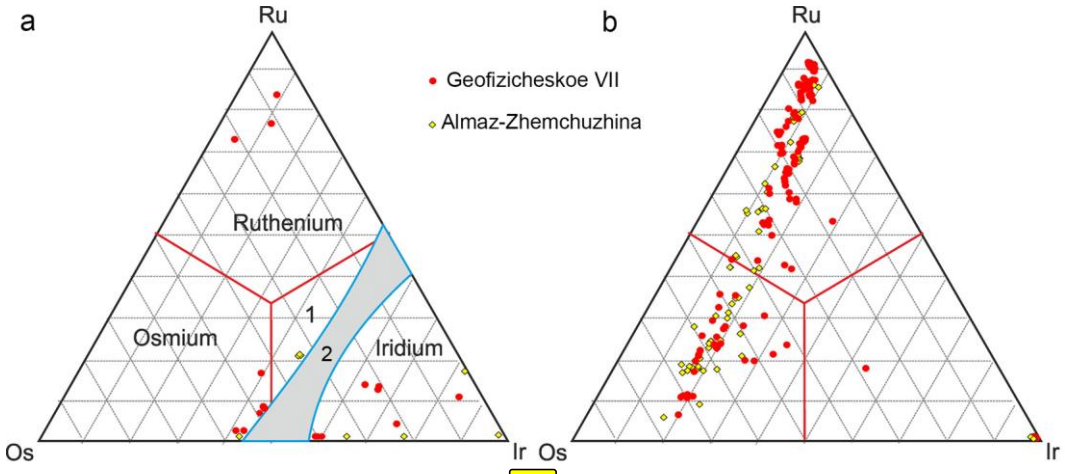

Figure 9. Compositions of PGM solid-solutions and sulfides in chromitites from the Almaz-Zhemchuzhina and Geofizicheskoe-VII deposits **(a)** Os-Ru-Ir alloys (at.%); **(b)** Os-Ru-Ir sulfides (at.%); (a) fields: 1 – rutheniridosmine, 2 – immiscibility area, after [33].

We must admit that the issue of the PGM inclusions genesis in chromite of podiform deposits makes constructing a simple model quite a challenge. At the same time, the segregations we studied show a number of similar features that suggest the leading role of subsolidus processes in their genesis. First, chromitites always display elevated concentrations of platinoids that keep growing from disseminated ores to massive ones. This fact is not consistent with "magmatic" models that release chromite and PGM from basaltoid melts [28]. On the contrary, it supports the first hypothesis about "preexisting elevated concentrations" of PGM in mantle chromite. Second, PGM inclusions are always enclosed within chromite grains, which contradicts the "fluid" genesis of mineralization. Third, objections to the solid-phase genesis due to the association of PGMs with hydroxyl-bearing phases dissaper once we assume that these associations are caused by the process of "impurity segregation" during the syntectonic recrystallization of chromite. All "exotic" mineral inclusions in the studied chromitite samples are clustered in serpentine, less often in a chlorite filling of the interstitial space, which most likely indicates their low-temperature genesis, simultaneously with the indicated secondary minerals.

5. Conclusions

The study of chromitites from the Dzharlybutak ore cluster deposits determined the following accessory minerals in inclusions from chromite grains, in addition to interstitial secondary minerals (serpentine, chlorite): 1) nominally anhydrous silicates (olivine, orthopyroxene, clinopyroxene), 2) hydroxyl-bearing silicates (amphibole, phlogopite, 3) base metal sulfides; 4) PGM. The interstices contain sulfides, arsenides, native minerals of Fe, Cu, Ni, Co, as well as such "exotic" minerals for ultramafic rocks and chromitite, as apatite, monazite, zircon, sphene, barite, and kassite.

Chromitites and host dunites occur as restite that was subject to transformation and rheomorphic differentiation within the mantle diapir. An intense depletion is evidenced

from the high magnesian (Fo[illegible]) and anomalously nickel-rich (up to 1.8 wt.% NiO) composition of olivine inclusions. Based on the composition of coexisting olivine and chromite, the temperature conditions (700–85[illegible]) and oxygen fugacity (-1.04 … +2.8 ΔFMQ) at the closing of this exchange reaction were estimated. They most likely indicate the completion of high-temperature processes in the upper mantle settings of the fore-arc basin.

We associate formation of inclusions of hydroxyl-bearing minerals (amphibole, phlogopite) in inner parts of ore grains with their capture at the early stages of the formation of Cr-spinel caused by decomposition of deformed pyroxenes of lherzolites and harzburgites [34]. Subsequent formation of chromitites followed the mechanism of rheomorphic differentiation within a localized zone of plastic flow (dunite). As a result, the inclusions were preserved inside a rigid chromite container.

[illegible]GM inclusions in inner parts of chromite grains were most likely formed under subsolidus conditions by IPGE atoms. The latter were incorporated in the Cr-spinel lattice at high mantle temperatures and segregated near defects and/or inclusions in result of cooling, plastic deformation, and recrystallization of the host mineral. Interstitial sulfides, sulfoarsenides and alloys of base metals and segregations of "exotic" minerals were produced by hydrothermal alteration of primary ultramafic rocks and chromitite.

Author Contributions: Conceptualization, methodology, writing, D.E.S; investigation, field work, sample preparation, D.E.S., D.K.M., R.A.G, writing—original draft preparation, D.E.S., R.A.G.; writing—review and editing, D.E.S.; visualization, D.E.S. and R.A.G., project administration, D.E.S.; funding acquisition, D.E.S. All authors have read and agreed to the published version of the manuscript.

Funding: This study was supported by the Russian Science Foundation grant no. 22-17-00019 (https://rscf.ru/project/22-17-00019/).

Data Availability Statement: The data presented in this study are available on request from the corresponding author.

Acknowledgments: The authors are very grateful to our colleagues from "[illegible]RC Exploration" Ischenko A.M., Khamzin A.B., Makat[illegible] Bastan K., Ulukpanov K.T., Alimov S. for [illegible]ul field trip on the Main Ore field deposits. We are grateful to T.A. Miroshnichenko for the English translation of our manuscript.

Conflicts of Interest: The authors declare no conflict of interest.

References

1. Gonzalez-Jimenez, J.M.; Griffin, W.L.; Proenza, A.; Gervilla, F.; O'Reilly, S.Y.; Akbulut, M.; Pearson, N.J.; Arai, S. Chromitites in ophiolites: how, where, when, why? Part II. The crystallisation of chromitites. Lithos 2014, 189, 148–158. https://doi.org/10.1016/j.lithos.2013.09.008
2. Pushkarev, E.V.; Kamenetsky, V.S.; Morozova, A.V.; Khiller, V.V.; Glavatskykh, S.P.; Rodemann, T. Ontogeny of ore Cr-spinel and composition of inclusions as indicators of the pneumatolytic–hydrothermal origin of PGM-bearing chromitites from Kondyor massif, the Aldan Shield. Geol. Ore Dep. 2015, 57, 352–380. https://doi.org/10.1134/S1075701515050049
3. Johan, Z.; Martin, R.F.; Ettler, V. Fluids are bound to be involved in the formation of ophiolitic chromite deposits. European Journal of Mineralogy. 2017, 29, 543–555. https://doi.org/10.1127/ejm/2017/0029-2648
4. Saveliev, D.E.; Fedoseev, V.B. Solid-state redistribution of mineral particles in the upwelling mantle flow as a mechanism of chromite concentration in the ophiolite ultramafic rocks (by the example of Kraka ophiolite, the Southern Urals). Georesources 2019, 21(1), 31–46. https://doi.org/10.18599/grs.2019.1.2-10
5. Borisova, A.Y.; Ceuleneer, G.; Kamenetsky, V.S.; Arai, S.; Béjina, F.; Abily, B.; Bindeman, I.N.; Polvé, M.; De Parseval, P.; Aigouy, T.; Pokrovski, G.S. A new view on the petrogenesis of the Oman ophiolite chromitites from microanalyses of chromite-hosted inclusions. J. Petrol. 2012, 53, 2411–2440. https://doi.org/10.1093/petrology/egs054
6. Distler, V.V.; Volchenko, Yu.A.; Kryachko, V.V.; Elpyshev, G.A.; Merkulov, G.A. PGM in chromitites of Kempirsai massif, the Southern Urals. Izvestiya AN USSR. Seriya Geol., 1987, 11, 113–117. (in Russian)
7. Distler, V.V.; Kryachko, V.V.; Yudovskaya, M.A. Formation conditions of PGE mineralization in chromium ores of Kempirsai ore field. Geology of Ore Deposits, 2003, 45, 44–74.
8. Distler, V.; Kryachko, V.; Yudovskaya, M. Ore petrology of chromite-PGE mineralization in the Kempirsai ophiolite complex. Miner. Petrol. 2008, 92, 31–58. https://doi.org/10.1007/s00710-007-0207-3
9. Dmitrenko, G.G. PGM in alpine-type ultramafic rocks. Magadan: Nauka, 1994. 134 p. (in Russian)
10. Thalhammer, T.V. Association of PGE minerals in massive chromite ores of the Kempirsai ophiolitic complex (the Southern Urals): Evidence for mantle metasomatism. Zapiski VMO, 1996, 125(1), 25–36. (in Russian)
11. Yurichev, A.N.; Chernyshov, A.I.; Korbovyak, E.V. Platinum group minerals from chromitites of Kempirsai ultramafic massif (the South Urals): new data. Zapiski RMO, 2019, 148(2), 76–86. https://doi.org/ 10.30695/zrmo/2019.1482.05
12. Melcher, F.; Grum, W.; Simon, G.; Thalhammer, T.V.; Stumpfl, E.F. Petrogenesis of the ophiolitic giant chromite deposits of Kempirsai, Kazakhstan: a study of solid and fluid inclusions in chromite J. Petrol. 1997, 38, 1419–1458. https://doi.org/10.1093/petroj/38.10.1419
13. Melcher, F.; Grum, W.; Thalhammer, T.; Thalhammer, O. A. R. The giant chromite deposits at Kempirsai, Urals: constraints from trace element (PGE, REE) and isotope data. Mineral. Deposita 1999, 34, 250–272. https://doi.org/10.1007/s001260050202
14. Melcher, F. Base metal – platinum-group element sulfides from the Urals and the Eastern Alps: characterization and significance for mineral systematics. Miner. Petrol. 2000, 68, 177–211. https://doi.org/10.1007/s007100050009
15. Leake, B.E.; Woolley, A.R.; Arps, C.E.S.; Birch, W.D.; Gilbert, M.C.; Grice, J.D.; Hawthorne, W.C.; Kato, A.; Kisch, K.J.; Krivovichev, V.G.; Lithout, K.; Laird, J.; Mandarino, J.A.; Maresch, W.V.; Nickel, E.A.; Rock, N.M.S.; Schumacher, J.C.; Smith, D.C.; Stephenson, N.C.N.; Ungaretti, L.; Whittaker, E.J.W.; Youzhi, G. Nomenclature of amphiboles; report of the subcommittee on amphiboles of the International Mineralogical Association commission on new minerals and mineral names. Canadian Mineralogist, 1997, 35, 219–246. https://doi.org/ 10.1127/ejm/9/3/0623
16. Whitney, D.L.; Evans, B.W. Abbreviations for names of rock-forming minerals. American Mineralogist, 2010, 95, 185–187. https://doi.org/ 10.2138/am.2010.3371
17. Kravchenko, G.G. The role of tectonics in the crystallization of chromite ores of the Kempirsay pluton. Nauka: Moscow, USSR, 1969; 232 p. (in Russian)
18. Kolotilov, L.I.; Kazantsev, M.M.; Razbaum, E.I. Structural and morphological zoning of ore clusters in the South Kempirsai chromite region, its prospecting and estimated value. Geology, metallogeny and material composition of ferrous metal ores in Kazakhstan. Alma-Ata, 1979, pp. 64–70. (in Russian)
19. Pavlov, N.V.; Kravchenko, G.G.; Chuprynina, I.I. Chromites of Kempirsay pluton. Nauka: Moscow, USSR, 1968; 178 p. (in Russian)
20. Grey, I.E.; Mumme, W.G.; Pekov, I.V.; Pushcharovsky, D.Y. The crystal structure of chromian kassite from the Saranovskoye deposit, Northern Urals, Russia. American Mineralogist, 2003, 88, 1331–1335. https://doi.org/ 10.2138/am-2003-8-916
21. Ballhaus, C.; Berry, R.F.; Green, D.H. High pressure experimental calibration of the olivine-orthopyroxene-spinel oxygen geobarometer: implications for the oxidation state of the upper mantle. Contr. Miner. Petrol. 1991, 107, 27–40. https://doi.org/10.1007/BF00311183
22. Ono, A. Fe-Mg partioning between spinel and olivine. Journal of Japanese Association of Mineralogy, Petrology and Economic Geology 1983, 78(4), 115–122. https://doi.org/10.2465/ganko1941.78.115
23. Roeder, P.L.; Campbell, I.H.; Jamieson, H.E. A re-evaluation of the olivine-spinel geothermometer. Contrib. Miner. Petrol. 1979, 68:325. https://doi.org/10.1007/BF00371554
24. Saveliev, D.E. Chromitites of the kraka ophiolite (south Urals, Russia): Geological, mineralogical and structural features. Mineral. Depos. 2021, 56, 1111–1132. https://doi.org/10.1007/s00126-021-01044-5.

25. Saveliev, D.E.; Makatov, D.K.; Portnov, V.S.; Gataullin, R.A. Morphological, textural and structural features of chromitite deposits of Main ore field of Kempirsay massif (South Urals, Kazakhstan). Georesursy, 2022, 24(1), 62–73. DOI: https://doi.org/10.18599/grs.2022.1.6
26. Saveliev, D.E.; Puchkov, V.N.; Sergeev, S.N.; Musabirov, I.I. Deformation-induced decomposition of enstatite in mantle peridotite and its role in partial melting and chromite ore formation. Doklady Earth Sciences, 2017, 476(1), 1058–1061. DOI: 10.1134/S1028334X17090161
27. Rakhimov, I.R.; Saveliev, D.E.; Vishnevskiy, A.V. Platinum metal mineralization of the South Urals magmatic complexes: geological and geodynamic characteristics of formations, problems of their genesis, and prospects. Geodynamics & Tectonophysics, 2021, 12 (2), 409–434. doi:10.5800/GT-2021-12-2-0531
28. González-Jiménez, J.M.; Griffin, W.L.; Gervilla, F.; Proenza, J.A.; O'Reilly, S.Y.; Pearson, N.J. Chromitites in ophiolites: How, where, when, why? Part I. A review and new ideas on the origin and significance of platinum-group minerals. Lithos, 2014, 189, 127–139. http://dx.doi.org/10.1016/j.lithos.2013.06.016
29. Gijbels, R.H.; Millard, H.T.; Deborough, G.A.; Bartel, A.J. Osmium, ruthenium, iridium and uranium in silicates and chromite from the eastern Bushveld Complex, South Africa. Geochimica et Cosmochimica Acta, 1974, 38, 319–337. https://doi.org/10.1016/0016-7037(74)90113-6
30. Naldrett, A.J.; Cabri, L.J. Ultramafic and related mafic rocks: their classification and genesis with special reference to the concentration of nickel sulfides and platinum-group elements. Economic Geology, 1976, 71, 1131–1158. https://doi.org/10.2113/gsecongeo.71.7.1131
31. Augé, T. Platinum-group mineral inclusions in ophiolitic chromitite from the Vourinos Complex. Greece. Canadian Mineralogist, 1985, 23, 163–171.
32. Gervilla, F.; Proenza, J.A.; Frei, R.; González-Jiménez, J.M.; Garrido, C.J.; Melgarejo, J.C.; Meibom, A.; Díaz-Martínez, R.; Lavaut, W. Distribution of platinum-group elements and Os isotopes in chromite ores from Mayarí-Baracoa Ophiolilte Belt (eastern Cuba). Contrib. Miner. Petrol., 2005, 150, 589–607. https://doi.org/ 10.1007/s00410-005-0039-2
33. Harris, D.C.; Cabri, L.J. Nomenclature of platinum-group-element alloys: review and revision. Canadian Mineralogist, 1991, 29, 231–237.
34. Saveliev, D.E.; Shilovskikh, V.V.; Sergeev, S.N.; Kutyrev, A.V. Chromian spinel neomineralisations and the microstructure of plastically deformed ophiolitic peridotites (Kraka massifs, Southern Urals, Russia). Min. Petrol. 2021, 115(4), 411–430. https://doi.org/10.1007/s00710-021-00748-w